



Steel Moment Resisting Frames with Sliding Hinge Joint Connections: Seismic Evaluation Using Various Response Indices

Paul Steneker¹, Lydell Wiebe², Andre Filiatrault^{3,4}

¹ Ph.D. Student, Department of Civil Engineering, McMaster University, Hamilton, ON, Canada

² Associate Professor, Department of Civil Engineering, McMaster University, Hamilton, ON, Canada

³ Professor, Department of Civil, Structural and Environmental Engineering, University at Buffalo State University of New York, Buffalo, NY, USA

⁴ Professor, University School for Advanced Studies IUSS, Pavia, Italy

ABSTRACT

Current methods of dissipating seismic energy in steel moment resisting frames rely on the plastic deformation of the beam sections near the column face. This type of deformation can deteriorate both the strength and stiffness of the connection and subsequently cause residual displacements within the structure after the end of the earthquake. A series of recently developed low damage connections, namely the sliding hinge joint and the self-centering sliding hinge joint, use friction rather than plastic deformations as the means of dissipating energy. Both connections use an asymmetrical friction connection as the energy dissipation mechanism, thereby maintaining the strength and stiffness of the connection at large rotations, and the self-centering sliding hinge joint also provides designers with the ability to select a level of self-centering force. Laboratory component tests of both joint types have been conducted, and these connections have been implemented in several structures in New Zealand. Hysteretic models that replicate the component behaviour of both connection types have previously been developed and used by the authors to determine the impact of these connections on the collapse performance of a six-storey frame. However, there is still a need to consider other complementary response indices, such as floor accelerations, residual displacements and the collapse performance during subduction or main shock-aftershock events.

This paper compares the performance of a six-storey steel moment resisting frame using four different types of connections: sliding hinge joint connections, self-centering sliding hinge joint connections, modern prequalified reduced beam section connections, and pre-Northridge connections that were common prior to the 1994 Northridge Earthquake and have limited ductility. The performance of these different versions of the frame is evaluated using five different response indices: (1) the maximum drift during a shallow crustal earthquake (2) the residual drift after a shallow crustal earthquake; (3) the maximum accelerations during a shallow crustal earthquake; (4) the maximum drift during a main shock-aftershock pair of shallow crustal earthquakes; and (5) the maximum drift during a longer duration subduction earthquake. The frame using self-centering sliding hinge joint connections provides the highest performance across all response indices, with the largest differences in performance being observed for the residual drifts and in the response to aftershocks and subduction earthquakes. This highlights the value of considering additional response indices beyond the maximum inter-storey drift for shallow crustal earthquakes.

Keywords: Steel Moment Resisting Frame, Low Damage Moment Resisting Connections, Sliding Hinge Joint, Performance Based Seismic Design, Subduction Ground Motion Performance, Main-Shock/After-Shock Performance

INTRODUCTION

The investigations following the 1994 Northridge Earthquake in California exposed the lower than expected performance of welded connections in steel moment resisting frames (MRFs) [1]. These observations resulted in a major research effort to develop reliable MRF connections that would be pre-qualified for use in seismic areas [2], examples of which are the reduced beam section (RBS), the welded stiffened end plate and the bolted flange plate. Designers may select among these prequalified connections when detailing steel MRFs [3] as existing component testing has ensured that these connections can undergo large amounts of plastic hinging, providing a reliable amount of hysteretic energy dissipation. However, this plastic

hinging can result in irrecoverable deformations in the beams, leading to the frame having significant residual displacements [4]. These residual displacements can cause large economic losses and significant delays in the operating capability of the structure [5].

To mitigate this issue, several low damage alternative connections have been proposed. Examples of such connections include the post-tensioned energy dissipating connections [6-7], connections using high-force-to-volume-dissipaters [8], the sliding hinge joint (SHJ) and its self-centering (SCSHJ) variant [9-10]. Each of these connections provides alternative energy dissipation methods but may require increases in detailing complexities when compared to the pre-qualified yielding connections. Among these proposed connections, this paper will focus on the effects of the implementation of the SHJ and the SCSHJ on the global seismic performance of MRFs.

The SHJ connection, initially proposed by Clifton [9], allows for a moment resisting frame to dissipate energy using an asymmetric friction connection placed at the bottom flange of the beam, dissipating energy via friction rather than plastic hinging. The asymmetric friction connection consists of bolts providing a normal force to a friction surface at the bottom of the beam web and the bottom beam flange. The top flange of the beam is connected to the column with a flange plate, allowing for the rotation of the beam about the top plate. A ring spring [11] can be added below the bottom beam flange of the SHJ connection to provide the self-centering behaviour of the SCSHJ connection [9]. The activation load and stiffness of the connection can be configured by modifying the friction surface properties, while the range of self-centering capability can be configured by modifying the ring spring. A series of full scale cyclic testing of these connections conducted by Khoo et al. [12] demonstrated their consistent energy dissipation and reliable self-centering capabilities.

With the recent shift towards performance based seismic design and particularly to seismic resiliency of structures, the low damage SHJ and SCSHJ connections provide designers with alternatives that may increase the overall performance of MRFs. The objective of this paper is to demonstrate the potential benefits of using newly developed low damage connections across multiple response indices. Using multiple engineering demand parameters (EDPs) and a variation in seismic hazards provides a better understanding of the impact of using low-damage connections when conducting performance based seismic design. A six-storey archetype steel MRF is analyzed with four different connection configurations: pre-Northridge connections (PRENORTH), pre-qualified reduced beam section connections (RBS), sliding hinge joint connections (SHJ), and self-centering sliding hinge joint connections (SCSHJ). The five distinct response indices are the maximum inter-storey drift and maximum accelerations during a shallow crustal ground motions, the maximum residual drift after a shallow crustal ground motion, the maximum inter-storey drift during a main-shock-after-shock (MS-AS) sequence of shallow crustal ground motions, and the maximum inter-storey drift during a subduction earthquake. These five indices were selected to capture the three distinct engineering demand parameters (EDPs) specified in ASCE-41 [13], as well as three different seismic hazards that are significant at the chosen site. All five response indices are evaluated at three different performance levels: immediate occupancy (IO), life safety (LS) and collapse prevention (CP) [13].

FRAME DESIGNS AND MODELLING APPROACH

The six-storey archetype frame model is shown in Figure 1 (a). This building was selected as it satisfies ASCE 7-16 design requirements for a location in Seattle, Washington on a site class B, which has spectral response parameters S_{DS} of 1.0g and S_{D1} of 0.4g [14]. The original building has a fundamental period of 1.3 seconds. The building was initially designed with RBS connections [15], and subsequent connection modifications consisted of changing the beam model hysteretic behaviour to match the respective connection properties, shown in Figure 1 (b). The yield moment of the PRENORTH connection was taken as that of the original beam without flange cuts, while the activation (yield) moment of the SHJ and SCSHJ connections were designed as 1/2 and 1/3 of the yield moment of the beam, respectively. A verification was conducted to ensure that all versions of the frame still satisfied the strong column/weak beam design principle at all locations.

The frame model was assembled in OpenSees [16] and consisted of elastic beam-column elements with concentrated rotational hinges at the ends. Each beam-to-column joint was modeled to capture panel zone yielding using the Krawinkler Spring box model [17], shown in Figure 1 (a), using a trilinear behaviour. For the PRENORTH and RBS connections, the beam and column hinges were modeled using the Ibarra-Medina-Krawlinker (IMK) model [18], resulting in the hysteresis loops shown in Figure 1 (b). The SHJ and SCSHJ beam connections were modeled using existing material models presented in previous research [19], and their corresponding hysteresis loops are shown in Figure 1 (b). A more detailed summary of the calibration of each beam connection is presented in Steneker et al. [19]. Equivalent Rayleigh damping of 2% was applied to each frame in the first and second elastic modes, mirroring common modeling practice. The Rayleigh damping was applied using a combination of mass proportional and constant stiffness proportional terms based on initial conditions. However, to avoid unrealistic and spurious damping forces, the stiffness proportional damping was determined using the approach proposed by Zareian and Medina [120]. No stiffness proportional damping was assigned to the Krawinkler spring box model

elements. The second order P- Δ effects were modeled with vertical loads consisting of the loads within the frame's lateral tributary area at each floor level, applied to a pin-connected gravity column shown in Figure 1 (a).

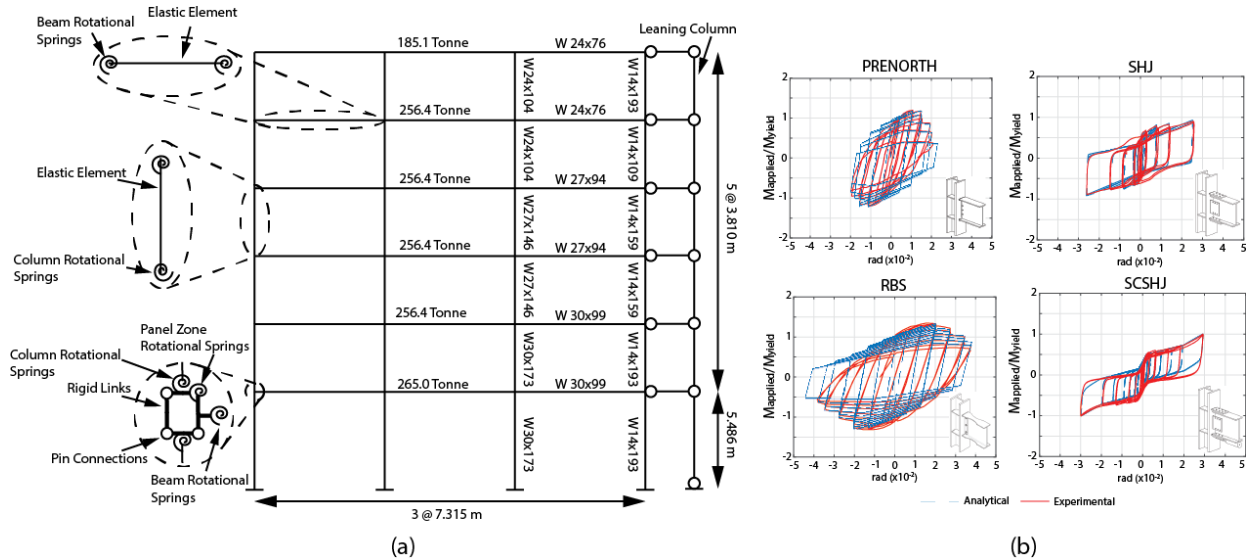


Figure 1. (a) Elevation view of six-storey archetype building model, (b) Hysteresis loops vs component tests results for all beam connection models

RESPONSE INDICES AND GROUND MOTION SELECTION

To understand the influence of the behaviour of each connection type on the overall frame performance, the frame described above was evaluated using five distinct response indices through a multiple stripe analysis [21]. Each multiple stripe analysis consisted of running non-linear time history analysis at seven intensities, each consisting of 40 individual ground motion components. These response indices were selected to quantify the performance of the frames under different seismic hazards and different EDPs. The evaluation of the performance of each frame was conducted at three performance levels identified in ASCE 41, immediate occupancy (IO), life safety (LS), and collapse prevention (CP) [13].

Response Indices 1, 2 and 3: Three EDPs for Shallow Crustal Ground Motions

The first three response indices were based on the response to typical shallow crustal ground motions selected from the NGA-West2 Database [22]. These motions were selected to match the dominant seismic hazard, having a magnitude varying from 6 to 7 and a rupture distance of 5 km to 50 km, as identified by the deaggregation data shown in Figure 2 (a) [23]. At each intensity stripe, the ground motions were selected and scaled to match the conditional mean spectrum at the first-mode period for each frame [24]. The median spectra for all intensity stripes, as well as the spectrum for each of the 40 ground motion components for the 1.0 MCE intensity (defined as a probability of exceedance of 2% in 50 years), are shown in Figure 2 (b).

The first response index, and the first of the three EDPs used for this particular seismic hazard, was the maximum inter-storey drift. The performance objective limits were defined by a maximum of 1% for IO, 2.5% for LS and 5% for CP [13]. The second response index was the maximum inter-storey residual drifts following the shallow crustal hazard. The maximum values for these residual drifts were taken as 0.1% for IO, 1% for LS and 2.5% for CP based on the recommendations of ASCE-41 [13]. The third response index for the single shallow crustal seismic hazard was the maximum floor acceleration during the ground motions, with maximum values of 0.5g for IO, 0.75g for LS and 1g for CP [13]. These values were determined by identifying the median accelerations of the corresponding damage state fragility curves of various non-structural office components defined in FEMA P-58 [5] based on the damage definitions in ASCE-41 [13].

Response Index 4: One EDP for Main-Shock-After-Shock Shallow Crustal Ground Motions

The fourth response index was evaluated for a different seismic hazard that represented a main-shock-after-shock (MS-AS) sequence of shallow crustal ground motions. For this hazard, the first motion consisted of the same shallow crustal motions selected previously from the NGA-West2 Database to match the conditional mean spectrum. These types of motions had a magnitude that varied from 6 to 7 and a distance ranging from near fault to 50 km, as specified by the deaggregation of seismic hazard shown in Figure 2 (a). The after-shock motion was selected using the targeted MS-MS procedure outlined in

Shokrabadi et al. [25], Goda [26] and Hatzigeorgiou and Beskos [27]. This procedure selects the AS ground motion from the library of main shock events but aimed to match the characteristics of magnitude and distance to an aftershock motion. This consisted of selecting motions with a lower magnitude and opposing rupture distance, examples of which consist of a MS event having a magnitude of 6.5 and rupture distance of 10.2 km to its AS counterpart with a magnitude of 5.5 and a distance of 39.8 km; or a MS event having a magnitude 6.8 and a distance of 42 km and its AS counterpart having a magnitude of 5.8 and a distance of 8 km. The selection and scaling of the aftershock records was conducted using the same conditional mean spectrum method but adjusting the selection parameters to match the AS ground motion characteristics mentioned above. Only one EDP evaluated for this hazard: the maximum inter-storey drifts of the frame, using the same limits as previously mentioned. This index was used to assess the general life-cycle resiliency of the frame when exposed to multiple motions.

Response Index 5: One EDP for Subduction Ground Motions

The fifth and final response index was the maximum inter-storey drift during a ground motion generated from a subduction type hazard. This seismic hazard originates from the Cascadia fault, located approximately 90 km from the archetype frame. This hazard is apparent in the deaggregation plots obtained from the United States Geological Survey (USGS), shown in Figure 2 (a) [23]. The subduction ground motions were selected from the K-NET database [28], as it has more records originating from subduction motions when compared to the NGA-West2 database. The scaling of the selected subduction ground motions was conducted using the same procedure that was described above for the selection of the shallow crustal ground motions, with the exception of using different magnitudes, distances and ϵ values due to the difference in hazard source [23]. The mean spectra for intensity stripes varying from 0.5 MCE to 3.0 MCE, and the individual spectra of the 40 subduction ground motions scaled to 1.0 MCE for the frame, are shown in Figure 2 (c).

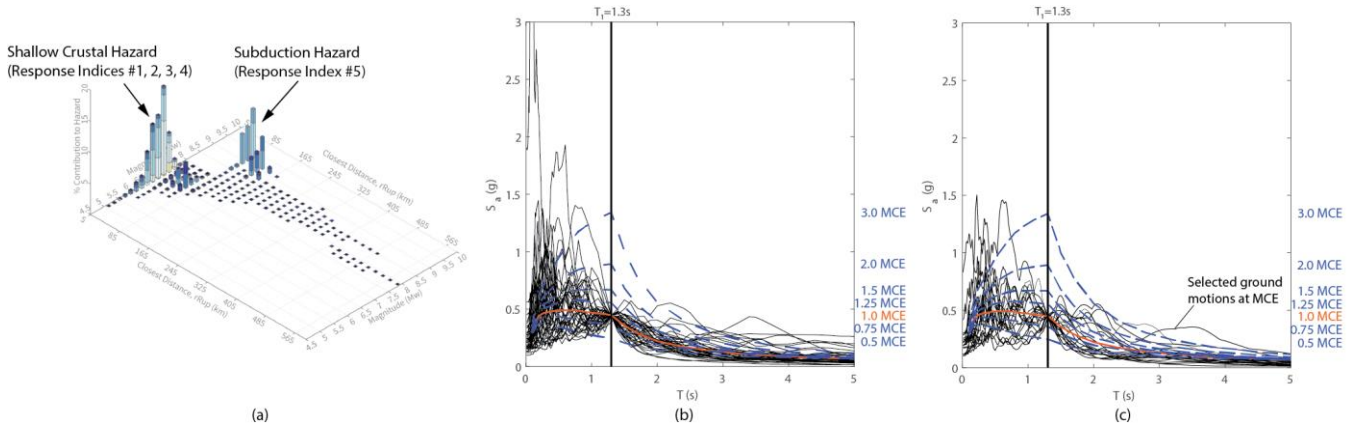


Figure 2. (a) Deaggregation of seismic hazard for Seattle site at 1 second (Modified from USGS [23]), (b) Shallow-crustal hazard conditional mean spectra, (c) Subduction hazard conditional mean spectra

PERFORMANCE OF FRAMES

For each stripe and for each response index, the percentage of the 40 ground motions causing the EDP in question to exceed the three limits corresponding to each of the three performance levels was determined. The maximum likelihood approach [21] was then used to fit a lognormal cumulative distribution function between the probability values of each stripe at each performance level. The resulting fragility curves are discussed below.

Results for Response Index 1: Maximum Inter-Storey Drifts for Shallow Crustal Ground Motions

Figure 3 shows the probability of exceedance for each frame type for the inter-storey drifts corresponding to the three performance level limits. The frame using only the PRENORTH connections has the lowest median intensity for each of the performance levels when compared to the other designs, with the largest difference at the CP level. The frame using only SCSHJ connections had the best overall performance at the CP performance level. However, the marginal increase in median performance at the CP level when changing the connections from PRENORTH to RBS is 88% greater than the improvement when changing the connections from RBS to SCSHJ. These differences in performance shrink at the lower performance levels, with the performances of all but the PRENORTH frame being essentially identical at the IO level. The frame using SHJ connections performed essentially identically to the frame with RBS connections, having a maximum increase in the median intensity of only 5% over the RBS frame, occurring at the CP performance level.

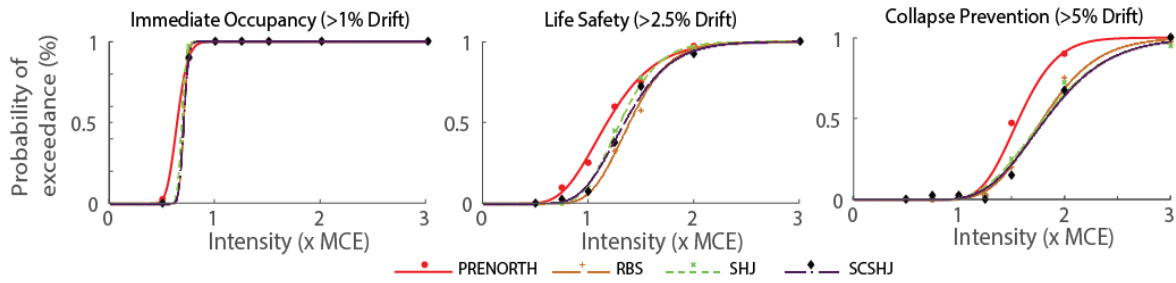


Figure 3. Fragility curves for inter-storey drifts after shallow crustal ground motions

Results for Response Index 2: Maximum Residual Inter-Storey Drifts for Shallow Crustal Ground Motions

Figure 4 shows the probability of exceedance for the residual displacements of the frame following shallow crustal ground motions. The order of the performance hierarchy remains consistent with those observed for the first response index. However, the differences in median intensities with different connection types are larger for this EDP when compared to those observed for maximum inter-storey drift (response index 1). The results indicate larger improvements in performance relative to using non-PRENORTH connections, with the SCSHJ frame having a median intensity of at least 25% larger than the PRENORTH frame for all three performance levels. However, the distribution of the curves are not as consistent, with the SCSHJ and SHJ frames having significantly larger improvements performance at intensities greater than their median intensity.

The reduction in median intensity for a single frame type when transitioning from a lower performance level (such as CP) to a higher performance level (such as IO) provides another indication of the performance gained with the use of the SCSHJ connection. The SCSHJ frame has half the average level-to-level reduction in median intensity as the reduction observed when using other connection types. This indicates that the self-centering behaviour of the SCSHJ connection results in no residual rotation for low intensity earthquakes. However, for the higher earthquake intensities, the residual displacements occur in the other frame components, such as the panel zones, beam hinges or column hinges. This was further confirmed by an element level analysis of these other frame components.

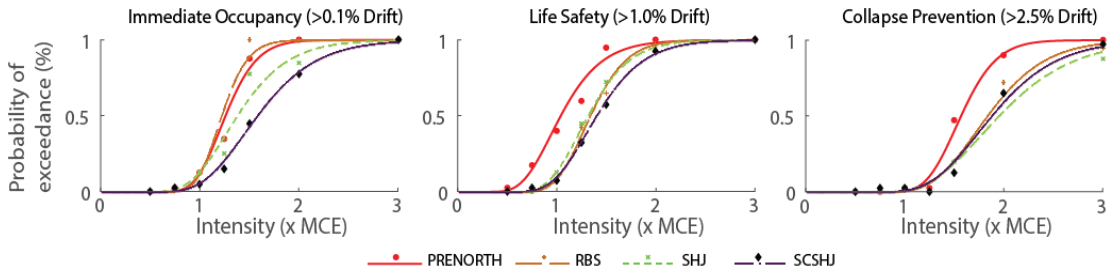


Figure 4. Fragility curves for residual inter-storey drifts during shallow crustal ground motions

Results for Response Index 3: Maximum Floor Accelerations for Shallow Crustal Ground Motions

The probability of exceedance for the maximum acceleration EDP for each of the frame versions at each performance level are shown in Figure 5. Since the elastic properties of each frame version were identical, the differences in acceleration are caused by the difference in yield moment and corresponding hysteretic behaviour. As observed for other response indices, the frame using SCSHJ connections once again has the best performance, while the PRENORTH frame has the lowest.

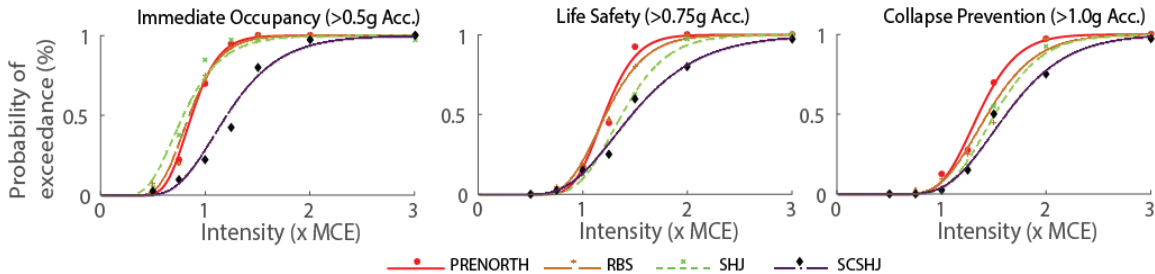


Figure 5. Fragility curves for accelerations during shallow crustal ground motions

Results for Response Index 4: Maximum Inter-Storey Drifts for MS-AS Shallow Crustal Ground Motions

For all four frame types, Figure 6 shows the probability of exceedance of the maximum inter-storey drift limits at all performance levels under the MS-AS shallow crustal ground motions. The hierarchy of performance remained similar to the previous results, with the PRENORTH frame having the worst performance, the SCSHJ frame having the best, and the RBS and SHJ frames having similar performance. The largest difference in performance occurred at the CP performance level, with a 50% increase in median intensity when changing from the PRENORTH to the SCSHJ connections.

A comparison of the results obtained from this response index to those obtained during response index 1 demonstrate that, when considering a second ground motion, the RBS frame has the largest overall reduction of the median intensity when compared to the other frame types. The reduction of median intensity caused by including the after-shock is 0.19xMCE for the RBS, 0.18xMCE for the PRENORTH, 0.17xMCE for the SHJ and 0.10xMCE for the SCSHJ frames. The lower reduction in performance for the SCSHJ frame with the addition of the second motion is due to the self-centering behaviour of the beam connection and the lack of stiffness and strength degradation. However, this improvement in performance is limited at larger ground motion intensities by the other frame elements, such as the panel zone, column hinge and secondary beam hinge, which yield at higher intensities.

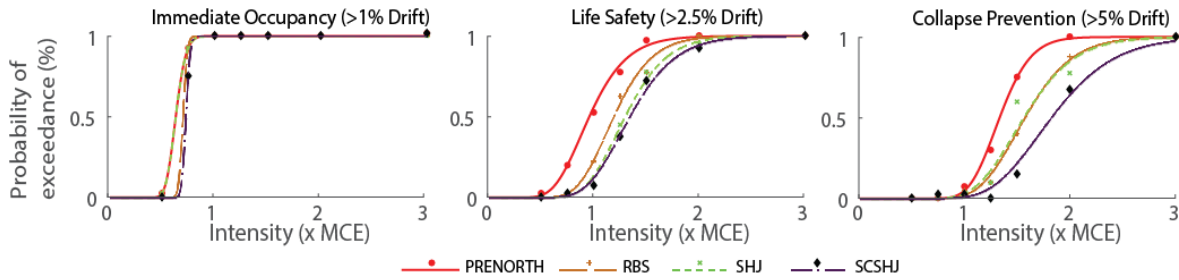


Figure 6. Fragility curves for inter-storey drifts during MS-AS shallow crustal ground motions

Results for Response Index 5: Maximum Inter-Storey Drifts for Subduction Ground Motions

For all frame types, the probability of exceedance for the maximum inter-storey drifts limits at all three performance levels under subduction earthquakes is shown in Figure 7. The performance of all frame types is significantly lower when compared to the same EDP using the shallow crustal motions. Furthermore, the uncertainty in the intensity causing collapse are all two times larger than those obtained for the shallow crustal motions. Nevertheless, the hierarchy of performance among the different connection types is consistent with what was observed for the previous response indices, with the SCSHJ frame having the highest overall performance and the PRENORTH frame having the lowest. Moreover, there are greater differences in performance among the different connection types for this index than for the others, particularly when considering the CP performance objective.

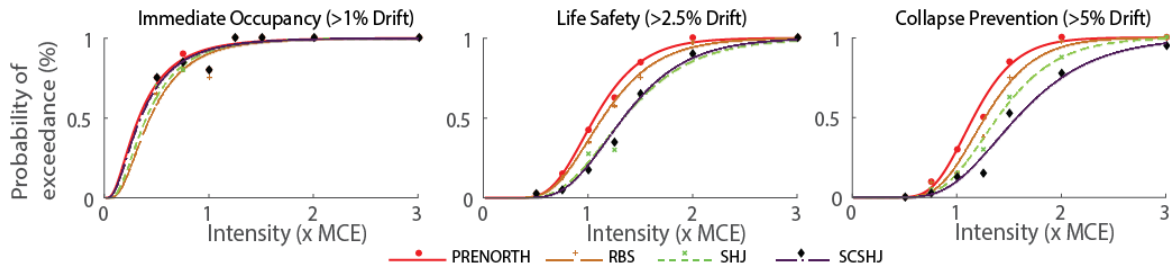


Figure 7. Fragility curves for inter-storey drifts during subduction ground motions

Overall Performance

Radar plots showing the median intensities obtained for all five responses indices were generated for each performance objective to allow for the visual comparison of the overall performance of each connection type. These are shown in Figure 8 for all four frame types. These plots demonstrate the overall gains in performance when using SCSHJ connections within a frame at the CP and LS performance levels. However, the gains obtained from using the SCSHJ connections are not as consistent across all response indices at the IO level: the improvements are significant for the acceleration and residual inter-storey drift response indices, but are negligible for the maximum inter-storey drifts during any of the three considered ground motion hazards. The performance of the SHJ frame generally fell between that of the RBS and SCSHJ frames, and had

particularly high performance for the acceleration and residual displacement response indices at the LS and CP levels. While the RBS frame performed better than the PRENORTH frame for all response index at the CP objective, these increases are not as significant or as consistent across the response indices at the LS performance, and are almost negligible at IO.

These plots can further demonstrate the relative strengths and weaknesses in performance of each frame type, allowing the identification of frames that have well balanced performance among the response indices considered in this research. An example is the SCSHJ frame for the LS performance objective, where each response index has a median probability of occurrence at approximately 1.5xMCE. A counter example is demonstrated by the same SCSHJ frame at the IO performance objective, as it has relatively high performance in the residual drift and acceleration response indices but lower performance in the other three indices. This balance in performance is a critical consideration when implementing performance based seismic design principles, as the omission of important EDPs or earthquake hazards can lead to the economic benefits of higher performance seismic force resisting systems being less than expected.

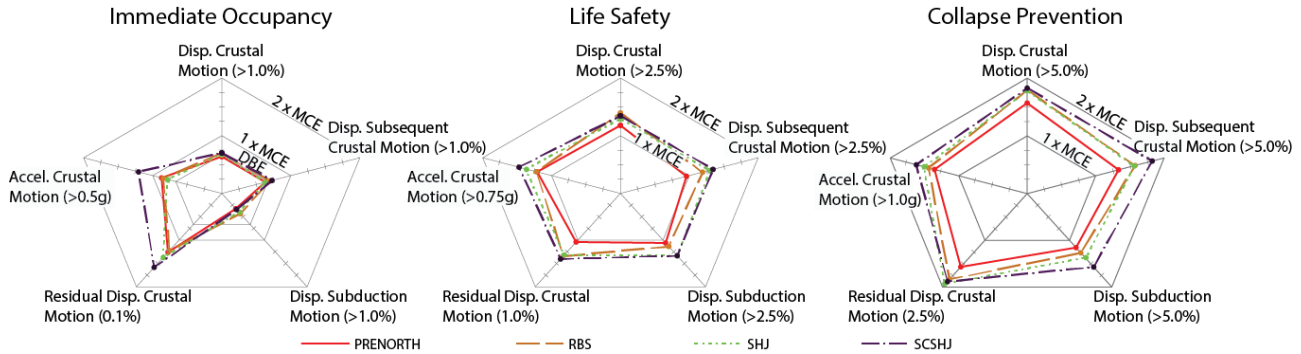


Figure 8. Summary graphs of median values for all frame types at three performance level limits

CONCLUSIONS

This paper presented the impact of two newly developed low damage moment resisting connections on the global performance of a six-storey moment resisting frame, across five response indices. The frame was evaluated with four different connection configurations: using pre-Northridge connections (PRENORTH), using pre-qualified reduced beam section connections (RBS), using sliding hinge joint connections (SHJ), and using self-centering sliding hinge joint connections (SCSHJ). Each response index was evaluated for three performance levels: Immediate Occupancy (IO), Life Safety (LS), and Collapse Prevention (CP). The frame using only PRENORTH connections had the lowest overall performance across all response indices and for all performance objectives. The frame using RBS connections had higher median intensities than the PRENORTH frame at the CP performance level only, having relatively similar median intensities to the PRENORTH frame at the lower performance levels. Whereas the performance of the frame using SHJ connections provided only marginal improvements over the performance of the frame using RBS connections, the frame using SCSHJ connections had the highest overall performance across all performance objectives and response indices. The potential increases in performance with the SCSHJ connections are readily apparent at the CP performance level during the shallow crustal earthquakes, and are even more apparent when examining accelerations, residual displacements, and displacements during longer duration ground motions or MS-AS scenarios. These results demonstrate the importance of considering non-traditional EDPs and loading scenarios when attempting to identify the potential economic advantages of using high performance seismic force resisting systems, such as SCSHJ connections. Further work could validate these trends in other frame configurations.

ACKNOWLEDGMENTS

The authors would like to acknowledge the assistance of Dr. Charles Clifton, Dr. Greg MacRae and Dr. Hsen-Han Khoo for providing component test data for the SHJ and SCSHJ connections. The authors would also like to acknowledge the National Science and Engineering Research Council (NSERC) for funding this research.

REFERENCES

- [1] Engelhardt, M. D. and Sabol, T. A. (1994). "Testing of welded steel moment connections in response to the Northridge earthquake." AISC Northridge Steel Update, (1).
- [2] Federal Emergency Management Agency (2000). "Recommended Seismic Design Criteria for New Steel Moment-Frame Buildings." FEMA-350.
- [3] American Institute of Steel Construction (2016). "AISC 358-16: Prequalified Connections for Special and Intermediate Steel Moment Frames for Seismic Applications."
- [4] Erochko, J., Christopoulos, C., Tremblay, R., and Choi, H. (2011). "Residual Drift Response of SMRFs and BRB Frames in Steel Buildings Designed according to ASCE 7-05." *Journal of Structural Engineering*, 137(5), 589–599.
- [5] Federal Emergency Management Agency (2012). "Seismic Performance Assessment of Buildings - methodology." Fema P-58-1, 1(September), 278.
- [6] Ricles, J., Sause, R., Garlock, M. and Krawinkler, H. (2001). "Posttensioned Seismic-Resistant Connections for Steel Frames." *Journal of Structural Engineering*, 127(2), 113–121.
- [7] Christopoulos, C., Filiatrault, A., Uang, C.-M., and Folz, B. (2002). "Posttensioned Energy Dissipating Connections for Moment-Resisting Steel Frames." *Journal of Structural Engineering*, 128(9), 1111–1120.
- [8] Mander, T.J., Rodgers, G.W., Chase, J.G., Mander, J.B. and MacRae, G.A. (2009). "Damage avoidance design steel beam-column moment connection using high-force-to-volume dissipaters." University of Canterbury Research Repository, 962.
- [9] Clifton, G.C. (2005) "Semi-Rigid Joints for Moment-Resisting Steel Framed Seismic-Resisting Systems." Retrieved from ResearchSpace@Auckland (Private Bag 92121)
- [10] Khoo, H.-H., Clifton, C., Butterworth, J., MacRae, G., Gledhill, S., and Sidwell, G. (2012). "Development of the self-centering Sliding Hinge Joint with friction ring springs." *Journal of Constructional Steel Research*, 78, 201–211.
- [11] Filiatrault, A., Tremblay, R. and Kar, R. 2000. "Performance Evaluation of Friction Spring Seismic Damper." *ASCE Journal of Structural Engineering*, 126(4), 491-499.
- [12] Khoo, H. H., Clifton, C., Butterworth, J., and Macrae, G. (2013). "Experimental study of full-scale self-centering sliding hinge joint connections with friction ring springs." *Journal of Earthquake Engineering*, 17(7), 972–977.
- [13] American Society of Civil Engineers (2017). "ASCE 41-17: Seismic Evaluation and Retrofit of Existing Buildings."
- [14] American Society of Civil Engineers (2016). "ASCE 7-16: Minimum Design Loads and Associated Criteria for Buildings and Other Structures."
- [15] Hall, J. (1995). "Parameter Study of the Response of Moment -Resisting Steel Frame Buildings to Near-Source Ground Motions." California Institute of Technology, Report No. EERL 95-08.
- [16] McKenna, F. and Scott, M. (2000). "Open system for earthquake engineering simulation."
- [17] Gupta, A. and Krawinkler, H. (1999). "Seismic Demands for Performance Evaluation of Steel Moment Resisting Frame Structures." (132), Department of Civil and Environmental Engineering, Stanford University, Report No. 132, 1–379.
- [18] Medina, R. and Krawinkler, H. (2005). "Strength demand issues relevant for the seismic design of moment-resisting frames." *Earthquake Spectra*, 21(2), 415–439.
- [19] Stenecker, P., Wiebe, L., Filiatrault, A. (2018) "A Comparison of Recently Developed Analytical Models for Steel Moment-Resisting Frame Connections" CSE Conference Proceedings, Fredericton, NB
- [20] Zareian, F., Medina, R. (2010). "A practical method for proper modeling of structural damping in inelastic plane structural systems." *Computers and Structures*, 88(1), 45-53.
- [21] Baker, J. W. (2015). "Efficient analytical fragility function fitting using dynamic structural analysis." *Earthquake Spectra*, 31(1), 579–599.
- [22] Chiou, B., Darragh, R., Gregor, N., and Silva, W. (2008). "NGA Project Strong-Motion Database." *Earthquake Spectra*, 24(1), 23–44.
- [23] United States Geological Survey (2008). "Unified Hazard Tool" (Lat: 47.6, Long: -122.3, T: 1.0 Sec)
- [24] Baker, J. W. and Lee, C. (2017). "An Improved Algorithm for Selecting Ground Motions to Match a Conditional Spectrum." *Journal of Earthquake Engineering*, 22 (4) 708-723.
- [25] Shokrabadi, M., Burton, H., Stewart, J. (2018) "Impact of Sequential Ground Motion Pairing on Mainshock-Aftershock Structural Response and Collapse Performance Assessment" *Journal of Structural Engineering*, 144(10)
- [26] Goda, K. (2012). "Nonlinear response potential of Mainshock-Aftershock sequences from Japanese earthquakes" *Bulletin of the Seismological Society of America*, 102 (5), 2139-2156.
- [27] Hatzigeorgiou, G. and Beskos, D. (2009) "Inelastic displacement ratios for SDOF structures subjected to repeated earthquakes" *Engineering Structures*, 31(11), 2744-2755.
- [28] Fujiwara, H., S. Aoi, T. Kunugi, and S. Adachi (2004). "Strong-motion observation networks of NIED: K-NET and KIK-net," *Cosmos Report*, National Research Institute for Earth Science and Disaster Prevention, Japan.